European Journal of Chemistry

View Journal Online
View Article Online

Crystallization of 3-hexulose-6-phosphate synthase

Masoud Delfi [1], Leila Mahdavian [2,*], Mohammad Sattarifar [2], Nina Hakulinen [1] and Juha Rouvinen [1]

[1] *Department of Chemistry, University of Eastern Finland, Joensuu Campus, Joensuu, FIN-80101 Finland*
masoud.delfi@unina.it (M.D.), nina.hakulinen@uef.fi (N.H.), juha.rouvinen@uef.fi (J.R.)
[2] *Department of Chemistry, Doroud Branch, Islamic Azad University, P.O. Box: 133. Doroud. Iran*
mahdavian_leila@yahoo.com (L.M.), m_sattari_1362@yahoo.com (M.S.)

* *Corresponding author at: Department of Chemistry, Doroud Branch, Islamic Azad University, P.O. Box: 133. Doroud. Iran.*
e-mail: mahdavian@iau-doroud.ac.ir (L. Mahdavian).

RESEARCH ARTICLE

10.5155/eurjchem.12.3.299-303.2072

Received: 18 January 2021
Received in revised form: 22 May 2021
Accepted: 15 July 2021
Published online: 30 September 2021
Printed: 30 September 2021

KEYWORDS

Protein crystallization
Formaldehyde fixation
Methylotrophic bacteria
Methylomonas aminofaciens 77a
3-Hexulose-6-phosphate synthase
Ribulose monophosphate pathway

ABSTRACT

The crystal structures can reveal detailed information about the overall structure, active site structure, and functional mechanism of enzymes. This study focused on the crystallization of 3-hexulose-6-phosphate synthase from *Methylomonas aminofaciens* 77a, to produce higher resolution crystals for precise structural characterization. 3-Hexulose-6-phosphate synthase is from *Methylomonas aminofaciens* 77a (EC 4.1.2.43). It belongs to the orotidine 5'-monophosphate decarboxylase superfamily, and acts as a key enzyme for a ribulose-monophosphate cycle of formaldehyde fixation and detoxification. 3-Hexulose-6-phosphate synthase catalyzes the aldol condensation of formaldehyde with D-ribulose-5-phosphate. For the maximum activity, 3-hexulose-6-phosphate synthase requires Mg^{2+} or Mn^{2+} as ligands. MaHPS crystallized at the concentration of 7 mg/mL and conditions consisting of 0.2 M $MgCl_2$, 18% PEG 3350 at pH = 7.0.

Cite this: *Eur. J. Chem.* **2021**, *12(3)*, 299-303 **Journal website**: www.eurjchem.com

1. Introduction

3-Hexulose-6-phosphate synthase (HPS) (EC 4.1.2.43) is an enzyme with a systematic name D-arabino-hex-3-ulose-6-phosphate formaldehyde-lyase (D-ribulose-5-phosphate-forming) [1]. 3-Hexulose-6-phosphate synthase from *Methylomonas aminofaciens* 77a, can be expressed in *E. coli*. The gene encoding MaHPS contains 624-bp open reading frame and is composed of 208 amino acid residues [2]. 3-Hexulose-6-phosphate synthase and 6-phospho-3-hexuloisomerase (PHI) are the key enzymes for formaldehyde fixation and detoxification in some specific methylotrophic bacteria by taking part in the ribulose monophosphate (RuMP) pathway [3]. In this prokaryotic pathway, formaldehyde-fixing enzymes (HPS and PHI) catalyze sequential reactions (Figure 1). The RuMP pathways consist of three main stages, i) fixation, ii) cleavage, and iii) rearrangement [3,4].

The crystal structure of HPS from the methylotrophic bacterium *Mycobacterium gastri* MB19 (*M. gastri* MB19) is available in Protein Data Base (PDB) with entry code 3AJX (Figure 2a). The crystal structure of HPS from *Methylomonas aminofaciens* 77a, has been found to share 44% amino acid sequence identity with HPS from *M. gastri* MB19. Also, the crystal structure of HPS from *Salmonella typhimurium*, StHPS, (PDB code 3F4W) has been determined as shown in Figure 2b. StHPS shares 39% amino acid sequence identity with HPS from *M. gastri* MB19 [5,6].

HPS from *M. gastri* MB19 shares ~30% amino acid sequence identity with 3-keto-L-gulonate-6 phosphate decarboxylase (KGPDC) from *E. coli*. MaHPS is from the orotidine 5'-monophosphate decarboxylase (OMPDC) superfamily. In PDB, 21 structures have been found to have a similar structure to 3-hexulose-6-phosphate synthase; seven examples which are from the OMPDC superfamily are given in Table 1. KGPDC and OMPDC share common conserved active site residues, which are used to catalyze their respective reactions [7]. However, there is no common reaction mechanism or substrate specificity among them [8].

The specific activity of 3-hexulose-6-phosphate synthase from *Methylomonas aminofaciens* 77a, under standard conditions, is 12.6 U/min.mg. The activity of 3-hexulose-6-phosphate synthase is affected by some parameters, such as pH and temperature. The highest enzymatic activity was observed to be at pH = 8.0 and T = 40 °C [9].

https://dx.doi.org/10.5155/eurjchem.12.3.299-303.2072

Table 1. Crystal structures of OMPDC superfamily enzymes extracted from PDB.

PDB code	Organism	Resolution	Year	Ligands
3AJX	*Mycobacterium gastri*	1.6 Å	2010	Sulfate ions, chloride ion, and magnesium
3JR2	*Vibrio cholerae*	1.8 Å	2009	Sulfate ion, glycerol, 1,2-ethanediol, and magnesium ion
3EXR	*Streptococcus mutans*	1.7 Å	2009	No ligand
3EXS	*Streptococcus mutans*	2.5 Å	2009	Ribulose-5-phosphate
3EXT	*Streptococcus mutans*	2.0 Å	2009	Magnesium ion
3IEB	*Vibrio cholerae*	2.1 Å	2009	Sulfate ion and glycerol
3F4W	*Salmonella enterica*	1.65 Å	2008	Malonate ion

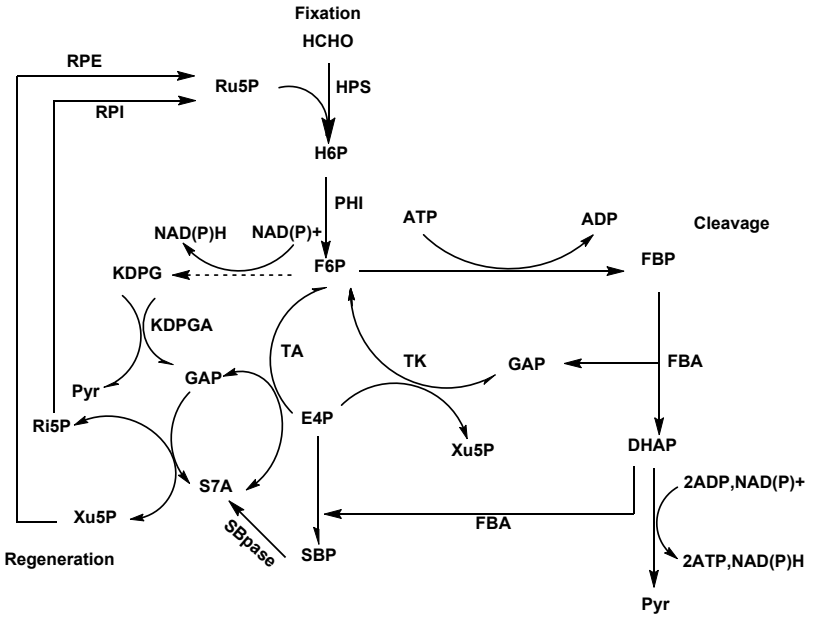

Figure 1. The sequential reactions catalyzed by HPS and PHI and outline of the three RuMP pathways [3].

Figure 2. The structure of 3-hexulose-6-phosphate synthase (a) from *M. gastri* MB19 and (b) from *Salmonella typhimurium*.

In the RuMP pathway, several reactions occur for formaldehyde fixation. The first step of the mentioned pathway is the catalysis reaction in which HPS plays a key role as a catalyst [10,11]. 3-Keto-L-gulonate-6-phosphate decarboxylase (KGPDC) and 3-hexulose-6-phosphate synthase, catalyze various reactions that share Mg^{2+}-assisted stabilization of 1,2-enediolate intermediates (Figure 3) [12]. KGPDC is involved in the metabolism of L-ascorbate by catalyzing the decarboxylation of 3-keto-L-gulonate 6-phosphate. In the formaldehyde fixation step, HPS catalyzes the aldol condensation of formaldehyde with D-ribulose 5-phosphate (Ru5P) in methylotrophic bacteria [9]. Structurally, KGPDC is a dimer of $(\beta/\alpha)_8$-barrel, having an active site on the interface of polypeptides [13]. At the C-terminal ends of the first, second, and third β-strands, there are conserved carboxylate groups which bind the Mg^{2+} leading to stabilization of the *cis*-1,2-enediolate intermediate produced by decarboxylation [6]. Then, the intermediate goes through a protonation process by two molecules of water which are located on the opposite faces of the intermediate, resulting in the final product, which is L-xylulose 5-phosphate. In the reaction catalyzed by HPS, Mg^{2+} coordinates with conserved homologues of the metal-ion ligands located in the active site of KGPDC. The conserved His stereo specifically abstracts a proton from the 1-hydroxymethylene group of D-ribulose 5-phosphate in order to generate D-arabino-hex-3-ulose 6-phosphate [14].

In this project, protein crystallization techniques were used to produce high-quality crystals of HPS that diffract in the X-ray beams very well with a satisfying resolution in order to study the three-dimensional structure and its functions.

2. Experimental

All chemicals used in this study are provided from Merck Co., Germany. Protein crystallization was performed by the hanging-drop vapor diffusion method in a 24-well cell culture plate (Greiner Bio-One, Austria). By pipette (Thermo scientific, Finland), mother-liquor, protein solution, and additives were transferred to the middle of siliconized glass circle cover slides (Hampton Research, USA). Then, the cover slides were placed inversely against reservoir buffer by tweezers and sealed by high vacuum grease (NSF, USA), to allow the equilibration between the protein droplet and mother liquor. All of the drops with different conditions were set according to the above-mentioned procedure.

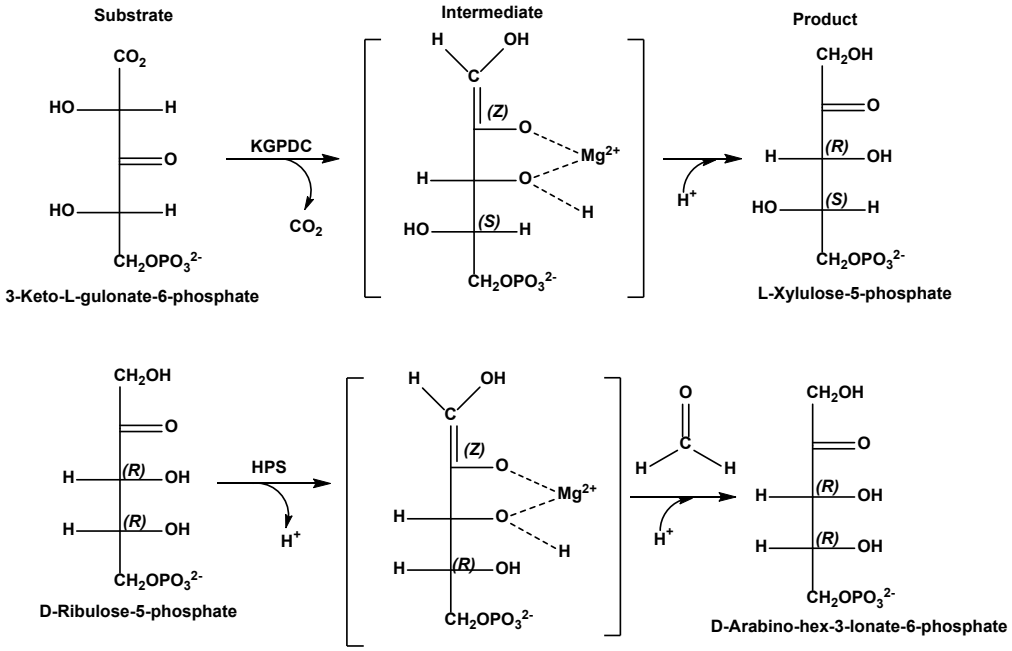

Figure 3. Reactions catalysed by KGPDC and HPS [12].

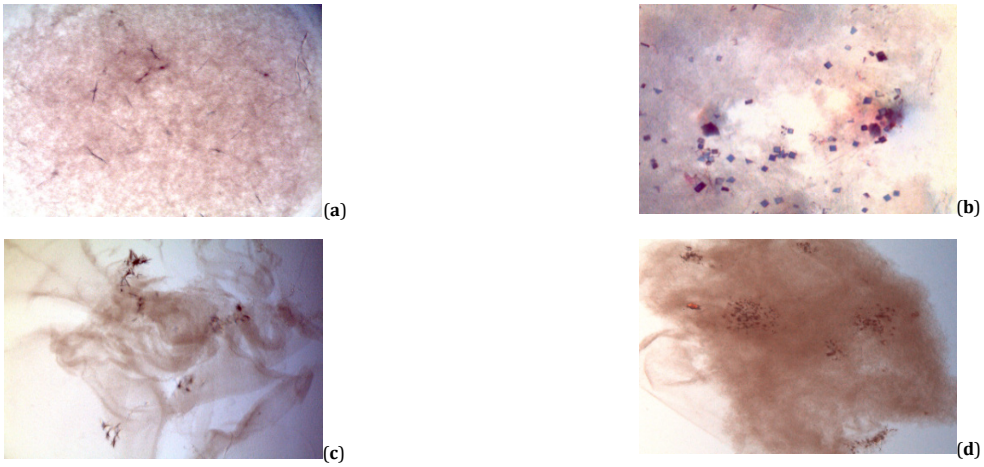

Figure 4. Crystals of MaHPS with screening CS-HR-1 & CS-HR-2. (a) Crystals appeared in the condition of 0.5 M ammonium acetate, 0.1 M tris pH = 8.5, 30% isopropanol at pH = 8.2 with 6 mg/mL MaHPS. (b) Crystals produced in the mother liquid containing 0.2 M magnesium acetate, 0.1 M tris pH = 8.5, 16% isopropanol at pH of 8.4 with 9 mg/mL MaHPS. (c) Crystals formed in the condition of 0.2 M magnesium acetate tetrahydrate, 0.1 M sodium cacodylate trihydrate at pH = 6.5, 25% MPD with 9 mg/mL MaHPS. (d) Crystals obtained in the condition including 0.2 M magnesium acetate tetrahydrate, 0.1 M sodium cacodylate trihydrate at pH = 6.5, 25% MPD with 9 mg/mL MaHPS and 3% ethanol as an additive.

3. Results and discussions

3.1. Crystallization of 3-hexulose-6-phosphate synthase from CS-HR-1 and CS-HR-2

For crystallization of 3-hexulose-6-phosphate synthase, CS-HR-1 & CS-HR-2 were screened. Three hits were found as result of these experiments. Medium size needle-like crystals appeared after 5 days with a condition consisting of 0.2 M ammonium acetate, 0.1 M tris pH = 8.5, 30% isopropanol at pH = 8.2 and a protein concentration of 6 mg/mL (Figure 4a).

Small cubic shape crystals appeared after 4 days of setting the drop in a condition including 0.2 M magnesium acetate, 0.1 M tris pH = 8.5, 16% isopropanol, at pH = 8.4. In this experiment, the concentration of protein was 9 mg/mL. When a crystal was tested with dye, it absorbed the dye as shown in Figure 4b. The grown crystals of this screening condition were fished by a mesh loop and sent for a diffraction test at a synchrotron radiation source. However, they did not diffract, which could be because of the low quality of crystals, packing process, and etc.

In addition, needle-like crystals appeared after 10 days as seen in Figure 4c, when crystallization condition consisted of 0.2 M magnesium acetate tetrahydrate, 0.1 M sodium cacodylate trihydrate pH = 6.5, 25% MPD. MaHPS was used with a concentration of 9 mg/mL. With 3% ethanol as an additive, the trial having 0.2 M magnesium acetate tetrahydrate, 0.1 M sodium cacodylate trihydrate pH = 6.5 and 25% MPD produced similar crystals after 5 days (Figure 4d) with 9 mg/mL MaHPS.

3.2. Crystallization conditions from CSS-1 and CSS-2

The crystallization was followed by screening CSS-1 and CSS-2 with 6 mg/mL MaHPS. Two hits were found from CSS-2. The first mother liquid contains 35% (*v*:*v*) 2-propanol, sodium cacodylate at pH = 6.5.

Figure 5. Crystals of MaHPS after screening of CSS-1 and CSS-2. Protein with the concentration of 6 mg/mL were used in both conditions. (a) Crystals appeared in the condition containing 35% (*v*:*v*) 2-propanol, sodium cacodylate at pH = 6.5. (b) Crystals seen in the condition including 40% (*v*:*v*) MPD, sodium cacodylate at pH = 6.5.

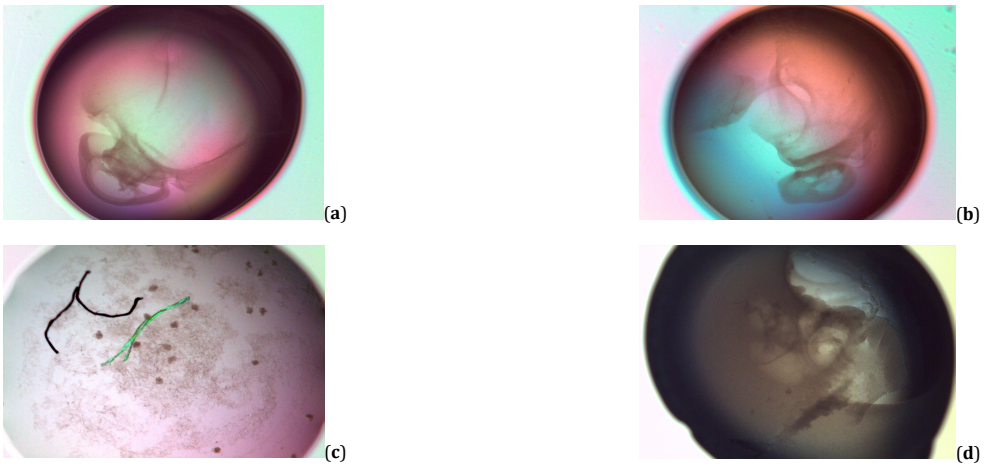

Figure 6. Crystal and diffraction results of MaHPS, the screening conditions consisted of 0.2 M $MgCl_2$, 18% PEG 3350 at pH =7.0. (a) with 6 mg/mL MaHPS. (b) With 9 mg/mL MaHPS. (c) With 12 mg/mL MaHPS. (d) With 15 mg/mL MaHPS.

Figure 7. Shows the crystal and diffraction results of MaHPS formed at the screening condition of 0.2 M $MgCl_2$, 18% PEG 3350 at pH = 7.0 with 7 mg/mL MaHPS and diffraction results.

The mentioned conditions resulted in large needle crystals after 12 days of screening as shown in Figure 5a. The next conditions which consisted of 40% (*v*:*v*) MPD, sodium cacodylate at pH = 6.5, produced needle crystals after 9 days (Figure 5b).

3.3. Effect of different protein concentration

Crystallization was performed by taking various protein concentrations (6, 9, 12, and 15 mg/mL) in the mother liquid consisting of 0.2 M $MgCl_2$, 18% PEG 3350 at pH = 7.0. The screened conditions with protein concentrations of 6, 9, 12, and 15 mg/mL led to precipitation as presented in Figure 6a-d.

While after 8 days of setting the same condition, a medium size crystal appeared (Figure 7), but this time MaHPS concentration was 7 mg/mL. To measure the quality of the crystal, it was fished and soaked in cryoprotectant, and immediately placed in liquid nitrogen. The conditions of cryoprotectant were 40% PEG 3350, 0.2 M $MgCl_2$ at pH 7.0. It was sent for diffraction by synchrotron radiation; however, it did not diffract (Figure 7).

4. Conclusion

3-Hexulose-6-phosphate synthase is an enzyme from *Methylomonas aminofaciens* 77a, and can be expressed and produced in *E. coli* [2]. This enzyme palys a key role in the Ribulose Monophosphate (RuMP) pathway for formaldehyde detoxification by assimilation into fructose-6-phosphate [3,4]. In order to discover the 3D structure of 3-hexulose-6-phosphate synthase, we performed a series of crystallization trials on these enzymes using hanging-drop vapor diffusion method. We first used two commercial kits, CS-HR-1 & CS-HR-2, to crystallize the enzyme. As a matter of fact, different types of crystals were obtained including needle crystals and small cubic shape crystals, although cubic crystals did not diffract at all (Figure 4). Again, crystallization trials were carried on by screening to other commercial kits, CSS-1 and CSS-2, on 3-hexulose-6-phosphate synthase. According to the observed data, only large-sized crystals were found in the crystallization drops (Figure 5). Finally, a promising crystallization condition consisting of 0.2 M $MgCl_2$, 18% PEG 3350 at pH = 7.0 were monitored in different protein concentrations i.e. 6, 9, 12, and 15 mg/mL. Interestingly, after 8 days of running a big size crystal formed in of 0.2 M $MgCl_2$, 18% PEG 3350 at pH = 7.0, and

protein concentration of 6 mg/mL, however, the crystal did not diffract (Figure 7). We believe that these crystallization trials on 3-hexulose-6-phosphate synthase are the first step toward characterization of 3-hexulose-6-phosphate synthase, and this work should be continued in this direction.

Acknowledgements

We would like to thank Department of Chemistry, University of Eastern Finland, Joensuu Campus, Joensuu, FIN-80101 Finland.

Disclosure statement

Conflict of interests: The authors declare that they have no conflict of interest.
Author contributions: All authors contributed equally to this work.
Ethical approval: All ethical guidelines have been adhered.

ORCID

Masoud Delfi
https://orcid.org/0000-0001-5003-1241
Leila Mahdavian
https://orcid.org/0000-0001-9582-4667
Mohammad Sattarifar
https://orcid.org/0000-0002-3788-8838
Nina Hakulinen
https://orcid.org/0000-0003-4471-7188
Juha Rouvinen
https://orcid.org/0000-0003-1843-5718

References

[1]. Stolzenberger, J.; Lindner, S. N.; Wendisch, V. F. *Microbiology* **2013**, *159* (Pt 8), 1770–1781.
[2]. Kato, N.; Yurimoto, H.; Thauer, R. K. *Biosci. Biotechnol. Biochem.* **2006**, *70* (1), 10–21.
[3]. Zhang, W.; Zhang, T.; Wu, S.; Wu, M.; Xin, F.; Dong, W.; Ma, J.; Zhang, M.; Jiang, M. *RSC Adv.* **2017**, *7* (7), 4083–4091.
[4]. Park, Y.; Yoo, H.; Song, M.; Lee, D.-H.; Lee, S. *Catalysts* **2018**, *8* (12), 582.
[5]. Orita, I.; Kita, A.; Yurimoto, H.; Kato, N.; Sakai, Y.; Miki, K. *Proteins* **2010**, *78* (16), 3488–3492.
[6]. Rahman, M. M.; Andberg, M.; Koivula, A.; Rouvinen, J.; Hakulinen, N. *Sci. Rep.* **2018**, *8* (1), 865.
[7]. Witthoff, S.; Schmitz, K.; Niedenführ, S.; Nöh, K.; Noack, S.; Bott, M.; Marienhagen, J. *Appl. Environ. Microbiol.* **2015**, *81* (6), 2215–2225.
[8]. Lee, J. C.; Herman, P. *Methods Enzymol.* **2011**, *488*, 185–217.
[9]. Kato, N.; Ohashi, H.; Hori, T.; Tani, Y.; Ogata, K. *Agric. Biol. Chem.* **1977**, *41* (7), 1133–1140.
[10]. Khurshid, S.; Saridakis, E.; Govada, L.; Chayen, N. E. *Nat. Protoc.* **2014**, *9* (7), 1621–1633.
[11]. Price, J. V.; Chen, L.; Whitaker, W. B.; Papoutsakis, E.; Chen, W. *Proc. Natl. Acad. Sci. U. S. A.* **2016**, *113* (45), 12691–12696.
[12]. Yew, W. S.; Wise, E. L.; Rayment, I.; Gerlt, J. A. *Biochemistry* **2004**, *43* (21), 6427–6437.
[13]. Wise, E.; Yew, W. S.; Babbitt, P. C.; Gerlt, J. A.; Rayment, I. *Biochemistry* **2002**, *41* (12), 3861–3869.
[14]. Yew, W. S.; Akana, J.; Wise, E. L.; Rayment, I.; Gerlt, J. A. *Biochemistry* **2005**, *44* (6), 1807–1815.